

# Zn(II) Complexes of 6-Aminobenzothiazole-Based Schiff Bases: Synthesis, Spectroscopic Characterization, DNA Binding Studies and Biological Investigations

K. Jagadesh Babu

Department of Chemistry, Government Degree College, Parkal, Hanamkonda, Telangana-506164, India,

**Abstract:** - Two novel Zn(II) complexes derived from 6-aminobenzothiazole-based Schiff base ligands (HL<sub>1</sub> and HL<sub>2</sub>) were synthesized and comprehensively characterized using spectroscopic and analytical techniques, including mass spectrometry, FT-IR, UV-Vis spectroscopy and thermogravimetric analysis (TGA). The complexes, formulated as [Zn(HL)<sub>2</sub>(H<sub>2</sub>O)<sub>2</sub>], were found to exhibit a six-coordinate octahedral geometry. DNA-binding studies, carried out using electronic absorption and fluorescence spectroscopy, indicated an intercalative mode of interaction, with binding affinities following the order 1a > 2a. The complexes also demonstrated efficient DNA cleavage activity under oxidative and photolytic conditions, showing greater efficacy than the free ligands. In vitro cytotoxicity studies against A549 (lung cancer) and MCF-7 (breast cancer) cell lines revealed enhanced anticancer activity for the Zn(II) complexes. Furthermore, antimicrobial investigations confirmed that the metal complexes possess superior activity compared to their parent ligands.

**Keywords:** Zn(II) Metal complexes; DNA binding; Anti bacterial; Antifungal; cytotoxic activity.

## 1. INTRODUCTION

Coordination compounds have emerged as an important class of materials in medicinal chemistry owing to their broad therapeutic and diagnostic potential. The unique electronic configurations of transition metal ions enable fine-tuning of molecular properties that are often inaccessible to purely organic systems [1]. The biological activity of metal complexes is strongly influenced by their coordination geometry, redox behavior, and physicochemical characteristics, making ligand design a crucial factor in optimizing their performance [2]. In this context, multidentate ligands containing suitable donor atoms play a vital role in the construction of biologically active metal complexes.

Among various ligand systems, Schiff bases (imines), formed via the condensation of primary amines with aldehydes or ketones, constitute a versatile and extensively studied class due to their ease of synthesis, structural diversity, and strong coordination ability through nitrogen and oxygen donor sites [3,4]. Their transition metal complexes have attracted considerable attention because of their diverse biological activities, including antimicrobial, anticancer, antioxidant, and antiviral properties [5,6]. Notably, the interaction of metal complexes with DNA is recognized as a key mechanism underlying their anticancer activity, as such interactions can interfere with DNA replication and transcription, ultimately inducing apoptosis [7]. These interactions are commonly investigated using techniques such as electronic absorption spectroscopy, fluorescence quenching, viscosity measurements, and gel electrophoresis [8].

In addition to their anticancer potential, transition metal complexes have also shown promise in the treatment of metabolic disorders such as diabetes mellitus (DM), a chronic condition characterized by persistent hyperglycemia and associated complications including neuropathy, nephropathy, and retinopathy. The inhibition of carbohydrate-metabolizing enzymes, such as  $\alpha$ -amylase, by metal complexes represents a potential therapeutic strategy for glycemic control [9,10]. Furthermore, their ability to mitigate oxidative stress through enhanced antioxidant activity significantly contributes to their pharmacological relevance. Chelation of Schiff base ligands with biologically important metal ions such as Cu(II), Co(II), Ni(II) and Zn(II) has been shown to enhance biological activity by increasing lipophilicity and reducing polarity, thereby facilitating improved cellular uptake [11–13]. Although platinum-based drugs such as cisplatin are widely used in chemotherapy, their clinical application is often limited by severe side effects and the emergence of drug resistance, highlighting the need for safer and more effective alternatives [14–16].

In this context, the present study focuses on the synthesis, characterization, and biological evaluation of novel Zn(II) complexes derived from Schiff base ligands obtained through the condensation of 6-aminobenzothiazole with substituted salicylaldehydes, namely 5-bromo-2-hydroxy-3-methoxybenzaldehyde and 2-hydroxy-3,5-diiodobenzaldehyde. Particular emphasis has been placed on their thermal stability, antibacterial activity, cytotoxic potential, and DNA-binding interactions as a plausible mechanism of action.

## 2. MATERIAL AND METHODS:

### 2.1. Materials:

All of the preparatory materials and solvents were procured from Sigma-Aldrich, Merck, and Hi Media Ltd. The solvents used for the synthesis were thoroughly distilled and dried according to standard methods. The Supercoiled pBR322 DNA and CT-DNA were purchased from Genei in Bangalore, India, and kept at 4 °C. Double-distributed water was used to prepare all of the buffer solutions for the DNA binding and cleavage experiments.

### 2.2. Methods:

The elemental analysis (C, H, N and S) of all the synthesised compounds was performed using a Perkin-Elmer elemental analyzer. FT-IR spectra were recorded on the Perkin-Elmer Infrared Model 337 in the range 4000-250 cm<sup>-1</sup>. UV-Vis spectra of compounds were analysed on a Shimadzu UV-Vis 2600 spectrophotometer in DMSO solvent in the range between 200 and 800 nm. ESI mass spectra were recorded on an HP-LC mass spectrometer (Agilent Tech, USA). The metal content of the complexes was determined using atomic absorption spectroscopy with the GBC Avanta 1.0 AAS. The melting points of the compounds were determined on a Polmon instrument (model No.MP-96). The thermo gravimetric analysis (TGA) of all metal complexes were carried out in a dynamic nitrogen atmosphere with a heating rate of 10 °C min<sup>-1</sup> on a Shimadzu TGA-50H in the temperature range of 27–1200 °C. Fluorescence spectra were recorded on a Shimadzu RF-5301PC spectrofluorometer.

### 2.3. Synthesis of Schiff base Ligands (HL<sub>1</sub> and HL<sub>2</sub>):

The ligands **HL<sub>1</sub>** and **HL<sub>2</sub>** were synthesized according to a previously reported procedure [17, 18]. A hot methanolic solution of 6-aminobenzothiazole (10 mM) was magnetically stirred in a round-bottom flask. To this, an equimolar methanolic solution (10 mM) of either 3,5-dichlorosalicylaldehyde or 3-bromo-5-chlorosalicylaldehyde was added dropwise under continuous stirring. The reaction mixture was refluxed at 70–80 °C for 5 hours, and the progress of the reaction was monitored by thin-layer chromatography (TLC). Upon completion, the resulting solid product was isolated by filtration, washed thoroughly with petroleum ether followed by methanol, and dried in a vacuum desiccator over anhydrous CaCl<sub>2</sub> to obtain the corresponding Schiff bases. The synthetic route is illustrated in **Scheme 1**.

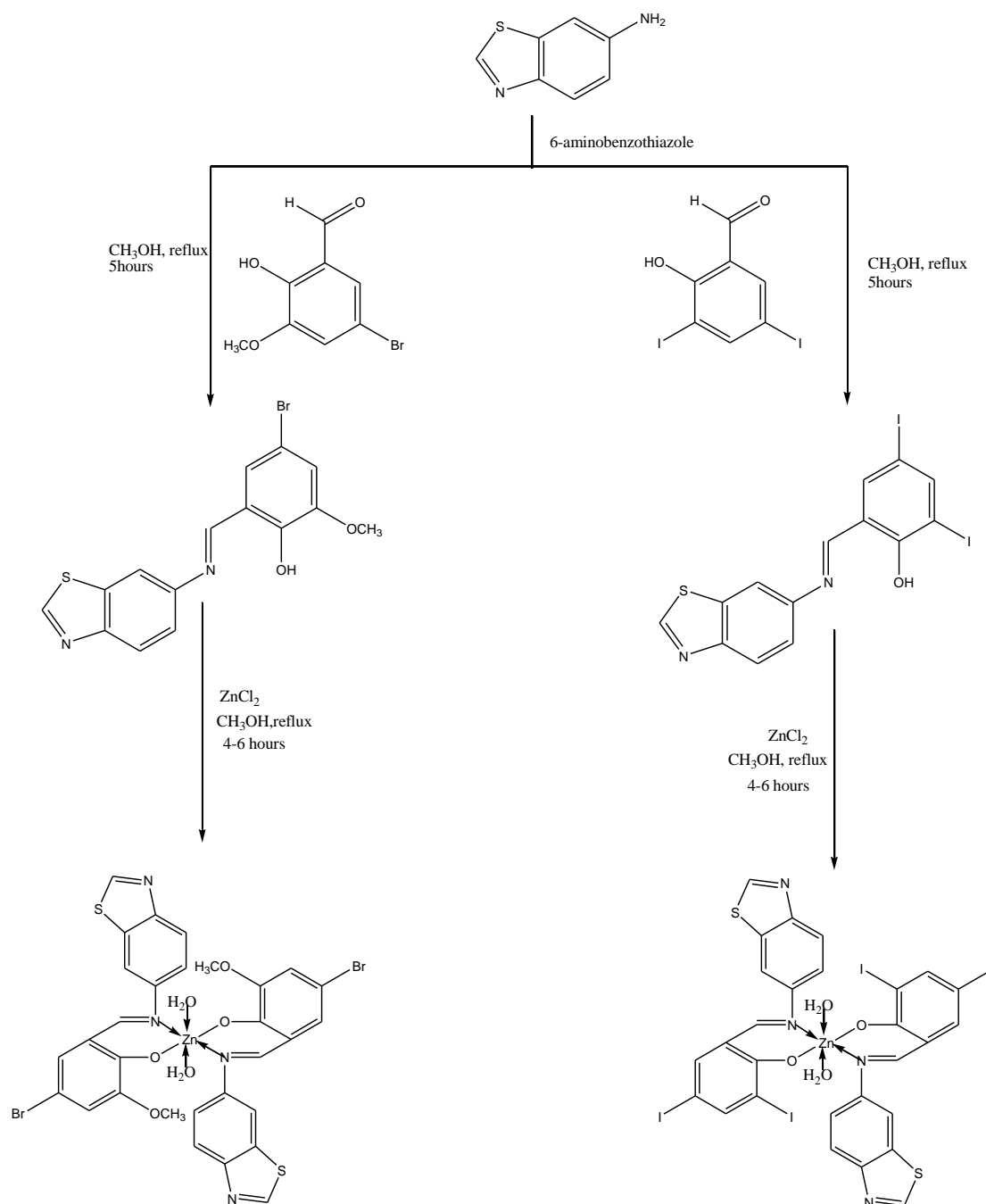
#### 2.3.1. 2-((E)-(benzo[d]thiazol-6-ylimino)methyl)-4-bromo-6-methoxyphenol

(C<sub>15</sub>H<sub>11</sub>BrN<sub>2</sub>O<sub>2</sub>S), (**HL<sub>1</sub>**):

Yield: 79%. Elemental Analysis. Calcd (%): Molecular formula C<sub>14</sub>H<sub>10</sub>N<sub>2</sub>O<sub>2</sub>S; Calculated: C, 49.60; H, 3.06; N, 7.71; S, 8.83. Found: C, 49.55; H, 3.01; N, 7.75; S, 8.78, **Melting Point**: 192-195 °C. IR (KBr): ν<sub>(OH)</sub> 3466, ν<sub>(HC=N)</sub> 1611, ν<sub>(C-O)</sub> 1255, (Fig. S1). UV-Vis: λ<sub>max</sub>/nm (cm<sup>-1</sup>): 256 (39062), 325 (30769), (Fig. S2). <sup>1</sup>H NMR (400 MHz, CDCl<sub>3</sub>) δ: 13.56 (s, 1H), 9.00 (s, 1H), 8.61 (s, 1H), 8.16 (d, *J* = 8.7 Hz, 1H), 7.84 (d, *J* = 2.0 Hz, 1H), 7.46 (dd, *J*<sub>1</sub> = 2.2, *J*<sub>2</sub> = 8.5 Hz, 1H), 7.16 (d, *J* = 2.0 Hz, 1H), 7.06 (d, *J* = 2.0 Hz, 1H), 3.92 (s, 3H), (Fig. S3). <sup>13</sup>C NMR (100 MHz, CDCl<sub>3</sub>) (δ): 161.8, 154.5, 152.4, 150.6, 149.4, 145.4, 135.0, 125.6, 124.3, 120.0, 119.7, 117.8, 114.4, 110.1, 56.4, (Fig. S4). LC-MS (m/z): Calc: 363.22: Found: 363 [M]<sup>+</sup> [18].

#### 2.3.2.2-((E)-(benzo[d]thiazol-6-ylimino)methyl)-4,6-diiodophenol (C<sub>14</sub>H<sub>8</sub>I<sub>2</sub>N<sub>2</sub>OS), (**HL<sub>2</sub>**)

Yield: 75%; Anal. Calc (%): C, 33.22; H, 1.59; N, 5.54; S, 6.34. Found: C, 33.15; H, 1.50; N, 5.60; S, 6.28; **Melting Point**: 185-190 °C. IR (KBr): ν<sub>(OH)</sub> 3451, ν<sub>(HC=N)</sub> 1621, ν<sub>(C-O)</sub> 1152, (Fig. S1). UV-Vis: λ<sub>max</sub>/nm (cm<sup>-1</sup>): 261 (38314), 324 (30864), (Fig. S2). <sup>1</sup>H NMR (400 MHz, CDCl<sub>3</sub>): δ: 14.42 (s, 1H), 9.02 (s, 1H), 8.53 (s, 1H), 8.19 (d, *J* = 8.7 Hz, 1H), 8.11 (s, 1H), 7.87 (s, 1H), 7.69 (s, 1H), 7.48 (d, *J* = 10.7 Hz, 1H), (Fig. S3). <sup>13</sup>C NMR (100 MHz, CDCl<sub>3</sub>): δ: 160.3, 160.1, 154.8, 152.7, 149.3, 144.6, 140.6, 135.1, 124.5, 120.6, 119.9, 114.6, 87.2, 80.1, (Fig. S4). ESI-MS (m/z): Calc: 506.10, Found: 505 (M-H)<sup>+</sup> [17].



**Scheme 1. Synthesis of Schiff base and corresponding 1a and 2a complexes.**

#### 2.4. Synthesis of binary metal complexes (1a-2a):

The Zinc metal complexes **1a** and **2a** were synthesized reacting the Schiff base ligands with the corresponding metal salts in a 1:2 (metal:ligand) molar ratio. A hot methanolic solution (10 mM) of ZnCl<sub>2</sub> was added dropwise to a hot, magnetically stirred methanolic solution of the Schiff base ligands (HL<sub>1</sub>/HL<sub>2</sub>) (20 mM). The reaction mixture was refluxed at 70–80 °C for 4–6 h with continuous stirring, and the progress of complex formation was monitored periodically. Upon completion, the resulting colored solid complexes were isolated by filtration, washed successively with hot methanol and petroleum ether to remove unreacted materials and impurities, and then dried in a vacuum desiccator over anhydrous CaCl<sub>2</sub>. The general synthetic route for the ligands and their corresponding metal complexes (1a and 2a) is illustrated in **Scheme 1**.

##### 2.4.1. [Zn(HL<sub>1</sub>)<sub>2</sub>(H<sub>2</sub>O)<sub>2</sub>]: (C<sub>28</sub>H<sub>22</sub>N<sub>4</sub>O<sub>6</sub>S<sub>2</sub>Zn) (**1a**):

Color: light orange Yield: 75%, M.pt: ~136 °C, Anal. Found. (Cal.) C, 43.12(43.63); H, 2.84 (2.93); Zn, 7.69 (7.92); N, 6.85 (6.78); S, 7.53 (7.77); IR (KBr) (cm<sup>-1</sup>):  $\nu$ (O-H) 3438;  $\nu$ (HC=N) 1617,  $\nu$ (C-O) 1243,  $\nu$ (M-O) 527,  $\nu$ (M-N) 472; 835, 765UV-Vis (DMSO)  $\lambda_{\text{max}}/\text{nm}$  (cm<sup>-1</sup>): 261 (38167), 330 (30303), 436 (20080);  $\mu_{\text{eff}}$  (BM): 0; MS (ESI): m/z 825.86 [M+2]<sup>+</sup> (**Figure 3. 1a**).

#### 2.4.2. [Zn(HL<sub>2</sub>)<sub>2</sub>(H<sub>2</sub>O)<sub>2</sub>]: (C<sub>28</sub>H<sub>18</sub>N<sub>4</sub>O<sub>4</sub>S<sub>2</sub>Zn) (2a):

Color: yellowish orange, Yield: 78%, M.pt: ~159 °C, Anal. Found. (Cal.) C, 30.01(30.25); H, 1.72 (1.63); Zn, 5.63 (5.88); N, 5.35 (5.04); S, 5.68 (5.77); IR (KBr) (cm<sup>-1</sup>):  $\nu$ (O-H) 3456;  $\nu$ (HC=N) 1615,  $\nu$ (C-O) 1138,  $\nu$ (M-O) 553,  $\nu$ (M-N) 467; 831, 734; UV-Vis (DMSO)  $\lambda_{\text{max}}/\text{nm}$  (cm<sup>-1</sup>): 257 (37593), 334 (32258), 476 (24096);  $\mu_{\text{eff}}$  (BM): 0; MS (ESI): m/z 1111.60 [M+H]<sup>+</sup> (**Figure 3. 2a**).

### 2.5. DNA binding studies:

#### 2.5.1. UV-Vis spectroscopic studies:

The DNA binding affinities of two monometallic complexes 1a and 1b were assessed using the UV-visible absorption method. The complex concentration maintained constant of 10  $\mu$ M, while the concentration of CT-DNA varied from 0 to 10  $\mu$ M. The complexes were initially dissolved in DMSO due to limited solubility in buffer solution. To prepare the CT-DNA stock solution, DNA was diluted in a Tris-HCl/NaCl buffer at pH = 7.2 (50mM NaCl/5 mM Tris-HCl). The purity of the CT-DNA was ensured by measuring UV spectra using molar extinction coefficient of 6600 M<sup>-1</sup> at 260 nm [17]. Mixing the CT-DNA solution with the respective complex and reference solution, followed by five minutes incubation before recording the absorption spectra. By analyzing the absorption data we determined the intrinsic binding constant (K<sub>b</sub>) for interaction of each complex with CT-DNA.

#### 2.5.2. Fluorescence quenching study:

Using fluorescence spectrophotometer and EB-bound CT-DNA in Tris HCl/NaCl buffer (pH 7.2), the binding between metal complexes and CT-DNA was investigated. The emission spectra of CT-DNA (125  $\mu$ M) bound to EB (12.5  $\mu$ M) were captured in the 360–800 nm region (350 nm excitation) as complex quantities were varied from 0 to 60  $\mu$ M. The comparative binding affinity of the complexes with CT-DNA was calculated using the quenching constant derived by the Stern-Volmer equation [18, 19],  $I_0/I = 1 + K_{\text{sv}} r$ . The fluorescence (emission band) intensities in the absence and presence of complexes are denoted by I<sub>0</sub> and I, respectively; K<sub>sv</sub> is a linear Stern-Volmer constant; and 'r' is the complex concentration as a proportion of the DNA concentration.

### 2.6. DNA cleavage:

The ability of schiff base and its monometallic metal compounds (1a, 1b and 1c) to cleave DNA was evaluated using agarosegel electrophoresis in the presence and absence of H<sub>2</sub>O<sub>2</sub>. Super coiled pBR322 DNA was diluted in a Tris-HCl/NaCl buffer at pH 7.2, and treated with varying concentrations of the metal complexes [20]. After a two hour incubation at room temperature, bromophenol blue (2 $\mu$ L) was added to the DNA sample followed by vigorous stirring. The sample was then loaded onto a 1% agarosegel containing a TAE buffer (PH 8.0) and subjected to electrophoresis at 70 V for 45 minutes. Prior to electrophoreses, the gel was stained with ethidiumbromide. The resulting gel is photographed using the BIO-RAD Gel documentation system, and the DNA bands were observed under transilluminators.

### 2.7. Biological Evaluation:

#### 2.7.1. Anti bacterial activity:

In vitro testing was using the agar well diffusion method to evaluate the antibacterial activity of all the compounds (HL<sub>1</sub>, HL<sub>2</sub> 1a and 2a) and the standard drug Gentamycin sulphate against two Gram positive (Staphylococcus aureus and Bacillus subtilis) and two Gram negative (Escherichia coli and Klebsiella pneumonia) bacterial stains. The bacterial culture was deposited on medium dishes after 24 hours of growth. Wells with three different concentrations (25, 50 75,  $\mu$ g/well) were created using a 6 mm cork borer. The plates were incubated at 25  $\pm$  2°C and inhibition zones were measured in mm and compared with the standard drug zones.

#### 2.7.2. Anti fungal activity:

Agarwell diffusion method was used to check in vitro anti fungal activity of synthesized compounds against two fungi species are Aspergillus niger and Candida albicans. One week old fungal culture was used as inoculums. Nystatin was used as reference antifungal drug. Antifungal data of compounds were expressed from the area of their inhibitory zone.

#### 2.7.3. Anticancer activity (MTT assay):

Synthesized substances (HL<sub>1</sub>, HL<sub>2</sub>, 1a, and 2a) were tested for their cytotoxicity on A-549 and MCF-7 cell lines. Cell viability was determined using the MTT assay. Tumour cells were cultured in 25 cm<sup>2</sup> flasks with appropriate medium at 37 °C in a CO<sub>2</sub> incubator. MCF-7 and A-549 cells were separately plated in a 96-well plate. After overnight growth, the cells were switched to low serum media. DMSO was used as the control. After 48 hours of exposure to different synthesized substances, the cells were treated with MTT solution for 4 hours. Then, the medium was removed. Optical density at 570 nm was measured using an ELISA plate reader, representing cell quantity. The results were reported as a percentage of cytotoxicity/viability. Every experiment was taken in triplicates, and the cytotoxicity of the test substance Doxorubicin was compared to determine the IC<sub>50</sub> values.

### 3. RESULTS AND DISCUSSION:

The Schiff base ligands and their corresponding metal complexes were successfully synthesized and characterized using spectral and elemental analyses. The synthesized Zn(II) complexes are colored, non-hygroscopic and stable at room temperature. They are soluble in DMF, DMSO, and acetonitrile, but insoluble in water. The obtained analytical data are in good agreement with the calculated values, confirming the proposed compositions. Furthermore, the results indicate that the metal-to-ligand stoichiometry in these complexes is 1:2.

#### 3.1. FT-IR Spectroscopy

FT-IR spectroscopy is a valuable technique for identifying functional groups and elucidating the coordination behavior of ligands with metal ions, including chelation and denticity. The FT-IR spectra of the Schiff base ligands and their metal complexes were recorded at room temperature over the range of 4000–250 cm<sup>-1</sup> using KBr pellets.

The Schiff base ligands HL<sub>1</sub> and HL<sub>2</sub> exhibited characteristic azomethine (C=N) stretching bands at 1611 and 1621 cm<sup>-1</sup>. Upon complexation, these bands shift by approximately 6 cm<sup>-1</sup>, indicating the participation of the azomethine nitrogen in coordination with the metal ion [21, 22]. A broad band observed at 3466 cm<sup>-1</sup> for HL<sub>1</sub> and 3451 cm<sup>-1</sup> for HL<sub>2</sub>, assigned to the phenolic –OH group, disappears after complexation, confirming the formation of a metal–oxygen (M–O) bond via the phenolic oxygen [23]. Moreover, the C–O stretching bands appear at 1255 cm<sup>-1</sup> for HL<sub>1</sub> and 1152 cm<sup>-1</sup> for HL<sub>2</sub>. In the metal complexes, these bands shift to slightly lower frequencies by 12–14 cm<sup>-1</sup>, further supporting coordination through the phenolic oxygen atom [22, 24]. New bands appearing in the regions 527–553 cm<sup>-1</sup> and 467–472 cm<sup>-1</sup> in the complexes are attributed to M–O and M–N stretching vibrations, respectively [25, 26]. A broad band observed at 3438 and 3456 cm<sup>-1</sup> in complexes 1a and 2a indicates the presence of coordinated water molecules within the coordination sphere [27]. Furthermore, an additional set of bands appeared in the range of 831–835 cm<sup>-1</sup> and 734–765 cm<sup>-1</sup>. These bands are attributed to the rocking and wagging vibrations, which further supports the existence of coordinated water molecules in the complexes.

These spectral features clearly demonstrate that the ligands coordinate to the metal ions in a bidentate manner through both azomethine nitrogen and phenolic oxygen atoms, as illustrated in **Figures 1.1a** and **1.2a**.

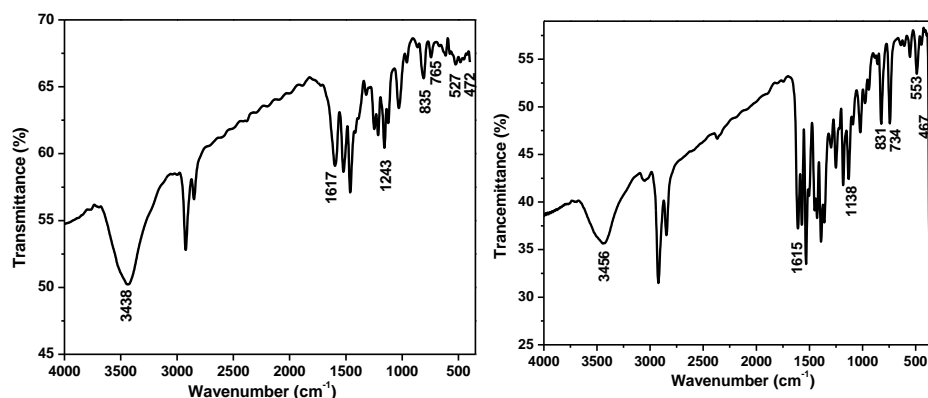


**Figure 1.** FTIR spectrum of metal complexes 1a, and 2a in the region of 4000-250 cm<sup>-1</sup>

#### 3.2. ESI Mass Spectral Studies

ESI mass spectrometry provides useful information about the molecular structure of a compound. The mass spectra of the metal complexes 1a and 2a showed molecular ion peaks at  $m/z = 825.86$  ( $[M+2]^+$ ) for 1a and  $m/z = 1111.60$  ( $[M+H]^+$ ) for 2a (**Figures 3. 1a** and **3. 2a**). These peaks confirm the formation of metal complexes with a  $[M(L)_2]$  composition. The mass spectral results, along with elemental analysis, support a 1:2 metal-to-ligand ratio in the complexes.

### 3.3. Electronic Spectra and Magnetic Moments

The electronic spectra of the synthesized Schiff base ligands HL<sub>1</sub> and HL<sub>2</sub> and their corresponding metal complexes (1a and 2a) were measured at room temperature using DMSO as the solvent. The spectral data are summarized in **Table 2** and depicted in **Figures 2. 1a** and **2. 1b**.

The free Schiff base ligands display two prominent absorption bands in the regions 256-261 nm (3906-38314 cm<sup>-1</sup>) and 325- 324 nm (3077-3086 cm<sup>-1</sup>), which are assigned to  $\pi \rightarrow \pi^*$  transitions within the aromatic rings and  $n \rightarrow \pi^*$  transitions of the azomethine (C=N) group, respectively [28]. In the metal complexes, these bands shifted to 261-257 nm (3831-3891 cm<sup>-1</sup>) and 330-334 nm (3030 -2994 cm<sup>-1</sup>), indicating coordination between the ligand and the metal ions [29]. Furthermore, an additional absorption band emerges in the region 436-476 nm (2293-2101 cm<sup>-1</sup>) in the metal complexes 1a and 2a respectively, which is absent in the free ligands. This band is attributed to ligand-to-metal charge transfer (LMCT) transitions [30]. Owing to the d<sup>10</sup> electronic configuration of Zn(II), d-d transitions are not observed in its complexes. The effective magnetic moments of complexes 1a and 2a are found to be zero, confirming their diamagnetic nature. Overall, these spectral characteristics support the successful coordination of the Schiff base ligands with the metal ions.

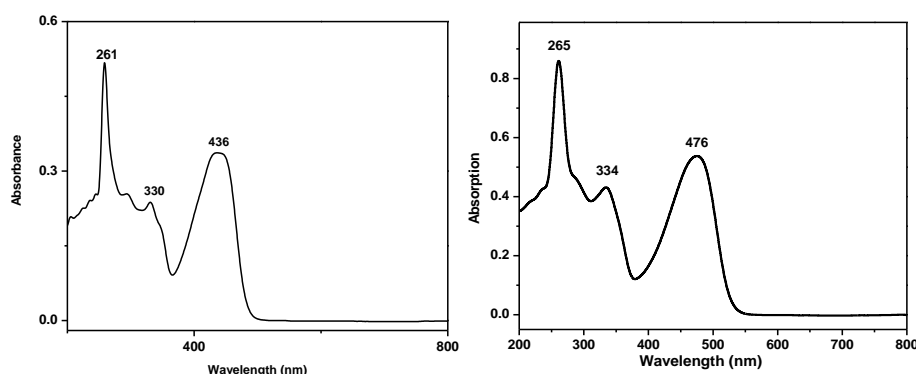


**Figure 2.** UV-Vis spectra of spectrum of metal complexes **1a**, and **2a** in the region of 200-800 nm.

### 3.4. Thermo gravimetric analysis:

Thermogravimetric analysis (TGA) of complexes 1a and 2a revealed a three-stage decomposition pattern (**Figure 4**). Both complexes remain thermally stable up to 121-139 °C, beyond which the first weight loss, observed between 121-196 °C, is attributed to the elimination of two coordinated water molecules. The second stage degradation, exhibiting a gradual mass loss for complex 1a in the range of 240-445 °C, whereas complex 2a shows a comparatively sharper weight loss between 270-580 °C, indicating partial degradation of the organic ligand framework in the metal complexes. The final stage, extending from 780 to 1053 °C, involves gradual mass loss in both complexes due to the complete decomposition of the organic moiety, ultimately leading to the formation of the corresponding metal oxide residue [22, 29].

Based on the combined interpretation of spectral studies and analytical data, the structures of the complexes are proposed as [Zn(HL<sub>1</sub>)<sub>2</sub>(H<sub>2</sub>O)<sub>2</sub>] for complex **1a** and [Zn(HL<sub>2</sub>)<sub>2</sub>(H<sub>2</sub>O)<sub>2</sub>] for complex **2a** (**Scheme I**).

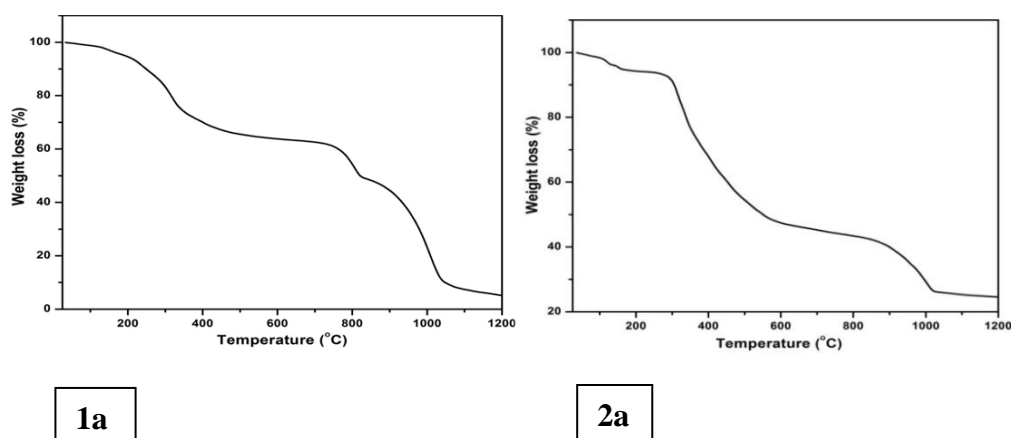


**Figure 4.** TGA curve of complex **1a**, and **2a**

### 3.5. DNA binding studies:

#### 3.5.1. Electronic absorption study:

In the current study, the interactions between CT-DNA and the metal complexes **1a** and **2a** were examined, and the changes in absorbance with and without CT-DNA are shown in Figure 4. Complexes **1a** and **2a** displayed absorption bands in the range of 261 and 265 nm, attributed to intra-ligand  $\pi-\pi^*$  transitions. Upon the addition of CT-DNA, a decrease in absorbance (hypochromism) along with a slight red shift (bathochromic shift) was observed, suggesting that the metal complexes interact with DNA through an intercalation mode [31-33]. To estimate the intrinsic binding constant ( $K_b$ ) of the complexes with CT-DNA, the equation  $[DNA]/(\epsilon_a - \epsilon_f) = [DNA]/(\epsilon_b - \epsilon_f) + 1/K_b(\epsilon_b - \epsilon_f)$  was used. In this equation,  $[DNA]$  is the concentration of CT-DNA (in base pairs),  $K_b$  is the intrinsic binding constant,  $\epsilon_a$  is the apparent molar absorptivity ( $A_{obsd}/[complex]$ ), and  $\epsilon_f$  and  $\epsilon_b$  are the molar extinction coefficients of the free and bound forms of the complex, respectively. The calculated binding constants were  $2.132 \pm 0.02 \times 10^5 M^{-1}$  for complex **1a** and  $1.635 \pm 0.02 \times 10^5 M^{-1}$  for complex **2a** [34, 35]. These findings confirm that both complexes have a strong binding affinity for CT-DNA, with complex **1a** showing greater binding strength than complex **2a**. (For comparison, ethidium bromide has a  $K_b$  of  $7 \times 10^7 M^{-1}$ ).

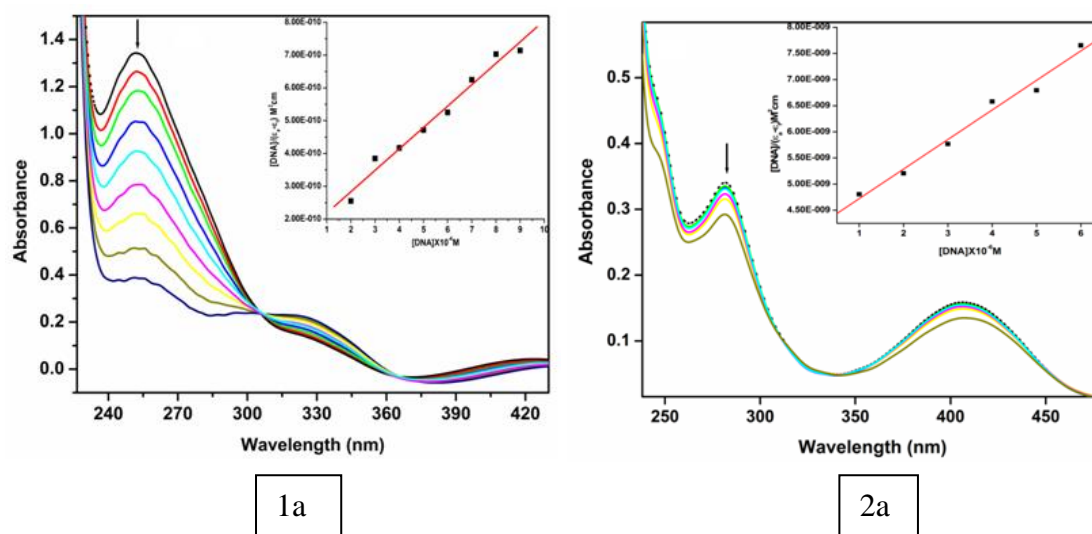


**Figure 5.** UV-Vis absorption spectra of complexes **1a** and **2a** in Tris-HCl buffer (pH 7.2) at 25 °C in the presence (solid line) and absence (dashed line) of an increase in concentration of CT-DNA. For the determination of the intrinsic binding constant,  $K_b$ , for DNA binding, see the inset linear plot.

#### 3.5.2. Fluorescence quenching study:

Fluorescence analysis using the emission intensity of the probe ethidium bromide (EB) was used to study the binding strength of metal complexes **1a** and **2a** with CT-DNA. In Tris-HCl buffer, EB shows weak fluorescence. When EB binds to CT-DNA by inserting between DNA base pairs (intercalation), its fluorescence intensity increases significantly [36, 37]. However, adding metal complexes to the EB-DNA system reduces this fluorescence, suggesting that the complexes compete with EB for DNA binding through an intercalative mode [38], as shown in **Figure 6**. The strongest emission of EB-DNA is observed between 587–592 nm. The Stern–Volmer quenching constants ( $K_{sv}$ ), obtained from fluorescence quenching data, revealed that complex **1a** has a higher binding affinity than **2a**. The  $K_{sv}$  values were  $1.9 \pm 0.02 \times 10^4 M^{-1}$  for **1a** and  $9.1 \pm 0.02 \times 10^3 M^{-1}$  for **2a**.

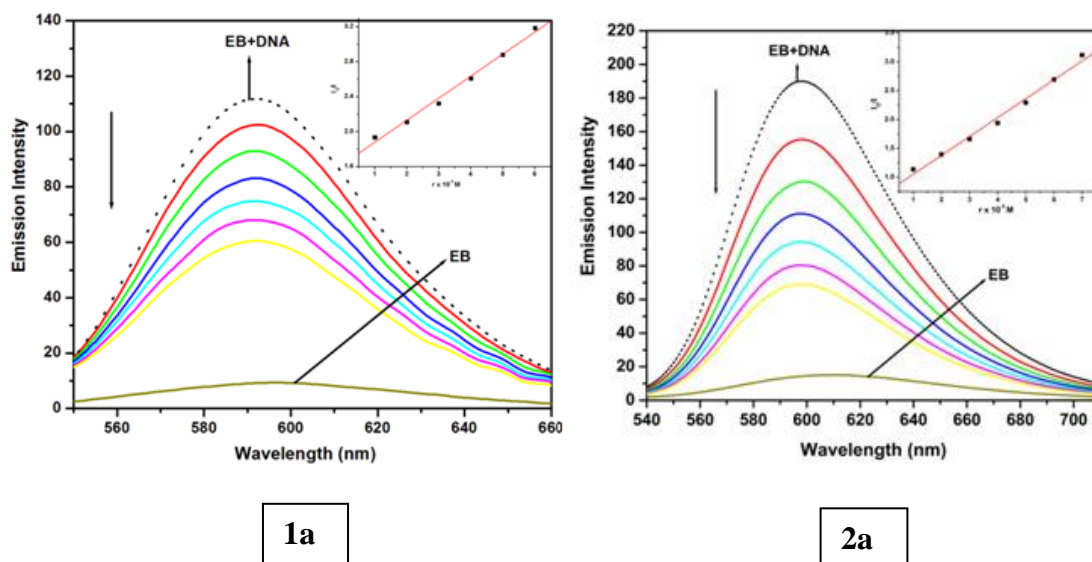


**Figure 6.** shows the fluorescence emission spectra of the CT-DNA-EB system at 25 °C with and without an increase in the concentration of the complexes 1a, and 2a in Tris HCl buffer (pH 7.2). When the concentration of the complexes grew, the emission intensity decreased, as seen by the arrow (↓). I<sub>0</sub>/I vs r inset.

### 3.6. DNA cleavage activity:

The interaction of pBR322 DNA with the Schiff base ligands HL<sub>1</sub> and HL<sub>2</sub>, along with their metal complexes **1a** and **2a**, was studied using gel electrophoresis under oxidative (with hydrogen peroxide) and photolytic (with UV light) conditions. DNA cleavage ability was assessed by tracking the transformation of supercoiled circular DNA (Form I) into nicked (Form II) and linear (Form III) forms. **Figures 7a and 7b** show the different DNA cleavage patterns observed during oxidative and photolytic treatments with HL<sub>1</sub>, HL<sub>2</sub>, and their metal complexes 1a and 2a. In the oxidative method (**Figure 7a**), the DNA control, DNA with H<sub>2</sub>O<sub>2</sub>, and ligands HL<sub>1</sub> and HL<sub>2</sub> (lanes 1–4) did not cause any noticeable DNA cleavage. In contrast, lanes 5 and 6, containing complexes 1a and 2a, showed effective conversion of supercoiled DNA (**Form I**) into the nicked form (**Form II**). Similarly, in the photolytic method (**Figure 7b**), the DNA control and both ligands (lanes 1-3) showed no cleavage. However, the presence of metal complexes in lanes 4 (1a) and 5 (2a) resulted in clear DNA strand scission, converting Form I into Form II [39].

These findings indicate that the metal complexes exhibit stronger DNA cleavage activity than the free ligands. This enhanced activity could be due to electron transfer from the donor atoms in the ligands to the positively charged metal ion, which may increase the lipophilicity of the complexes and improve their interaction with DNA [40].

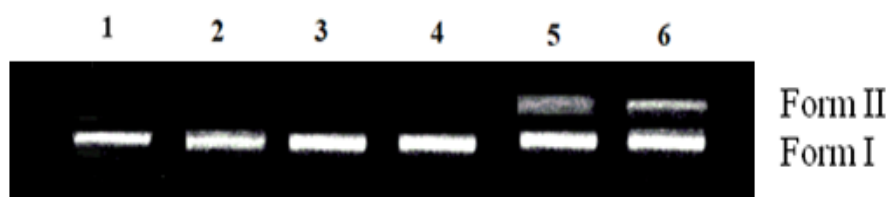


**Figure 7a.** The metal complexes oxidatively cleaved supercoiled pBR322 DNA (0.2 µg, 33.3 µM) at 37 °C in a buffer of 5 mM Tris HCl/5 mM NaCl. 1<sup>st</sup> lane, DNA control; 2<sup>nd</sup> lane, DNA + H<sub>2</sub>O<sub>2</sub> (1 mM); 3<sup>rd</sup> lane, DNA + H<sub>2</sub>O<sub>2</sub> (1 mM) + HL<sub>1</sub>; 4<sup>th</sup> lane, contains DNA + H<sub>2</sub>O<sub>2</sub>+HL<sub>2</sub>; 5<sup>th</sup> lane contains DNA + H<sub>2</sub>O<sub>2</sub> (1 mM) + 1a; 6<sup>th</sup> lane, contains DNA + H<sub>2</sub>O<sub>2</sub> (1 mM) + 2a.

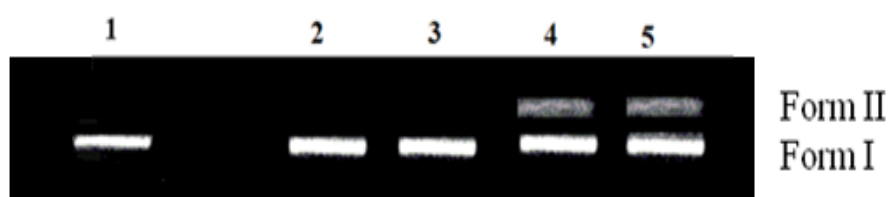


**Figure 7b.** Photoactivated cleavage of supercoiled pBR322 DNA by the complexes UV-light at 37 °C in 5 mM Tris HCl/5 mM NaCl buffer (long UV-365 nm). 1<sup>st</sup> lane, DNA control; 2<sup>nd</sup> lane, DNA + HL<sub>1</sub>; 3<sup>rd</sup> lane, DNA + HL<sub>2</sub>; 4<sup>th</sup> lane, DNA + 1a; 5<sup>th</sup> lane, DNA + 2a.

### 3.7. Biological studies:

#### 3.7.1. Anti bacterial activity:

The antibacterial activity of the synthesized Schiff base ligands HL<sub>1</sub> and HL<sub>2</sub>, along with their corresponding metal complexes 1a and 2a, was evaluated using the agar well diffusion method. As shown in **table 3** and **figure 8**, the metal complexes exhibited significantly higher antibacterial efficacy than their respective free ligands. This enhancement can be attributed to the chelation theory proposed by Tweedy, which suggests that metal coordination increases the biological activity of ligands. Among the tested compounds, complex 1a demonstrated the most potent inhibitory effect against both Gram-positive and Gram-negative bacterial strains, although its activity was lower than that of the standard drug.

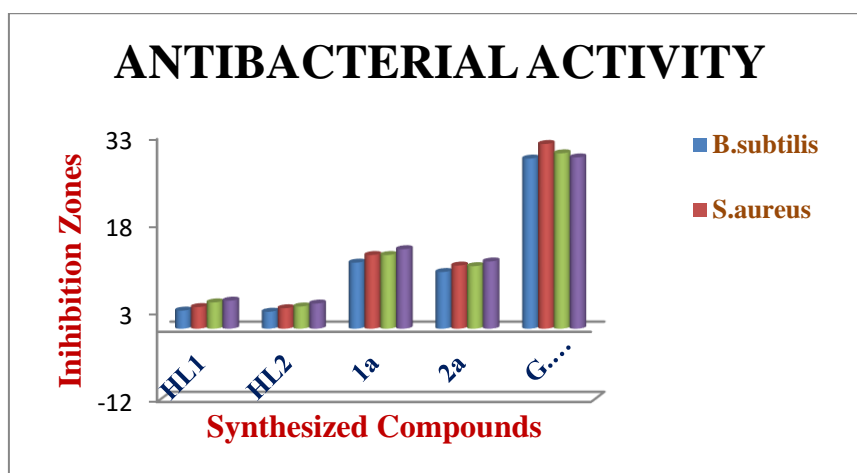


**Figure 8.** Graphical representation of the antibacterial activity of Schiff bases (HL<sub>1</sub> & HL<sub>2</sub>) and their metal complexes (1a & 2a)

#### 3.7.2. Antifungal activity:

The synthesized Schiff base HL<sub>1</sub> and HL<sub>2</sub> and their metal complexes (1a and 2a) were evaluated for their in vitro antifungal efficacy against two fungal strains, *Aspergillus niger* and *Candida albicans*. Their performance was benchmarked against the well-established antifungal agent nystatin at an equivalent concentration (see **Table 4** and **Figure 9**). The results indicated that the metal complexes displayed enhanced antifungal activity relative to the free Schiff base ligand. Among them, complex 1a demonstrated notably stronger antifungal effects than complex 2a. This increased activity may be ascribed to the presence of bromo group in the Schiff base ligand of complex 1a. However, it is important to note that the antifungal activity of these metal complexes remained lower than that of the standard drug nystatin.

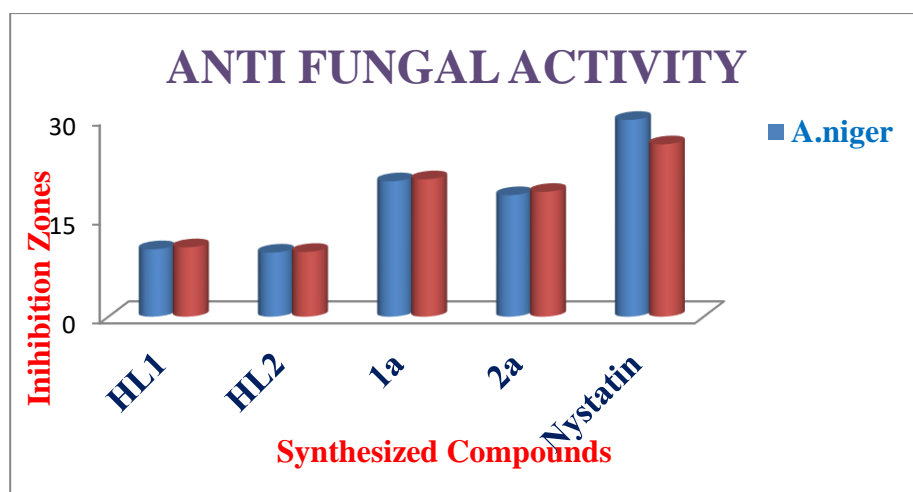


Figure 9. Graphical representation of anti-fungal activity of Schiff bases (HL<sub>1</sub> & HL<sub>2</sub>) and their metal complexes (1a & 2a)

### 3.7.3. Anticancer activity (MTT assay):

The anticancer activity of the Schiff base ligands HL<sub>1</sub> and HL<sub>2</sub>, along with their metal complexes 1a and 2a, was assessed using the MTT assay against MCF-7 (human breast cancer) and A-549 (human lung adenocarcinoma) cell lines. Doxorubicin, a well-established anticancer drug, served as the reference standard. The IC<sub>50</sub> values of all synthesized compounds are presented in **table 5** and **figure 10**. The cytotoxicity data indicated that all tested complexes exhibited significant cytotoxic effects against the MCF-7 cell line, surpassing their activity against the A-549 cell line. Among them, complex 2a exhibited the most pronounced cytotoxicity. Moreover, all metal complexes demonstrated enhanced activity compared to their corresponding free ligands, suggesting that metal coordination improved the anticancer potential of the compounds. The order of cytotoxicity was found to be HL<sub>1</sub> < HL<sub>2</sub> < 2a < 1a.

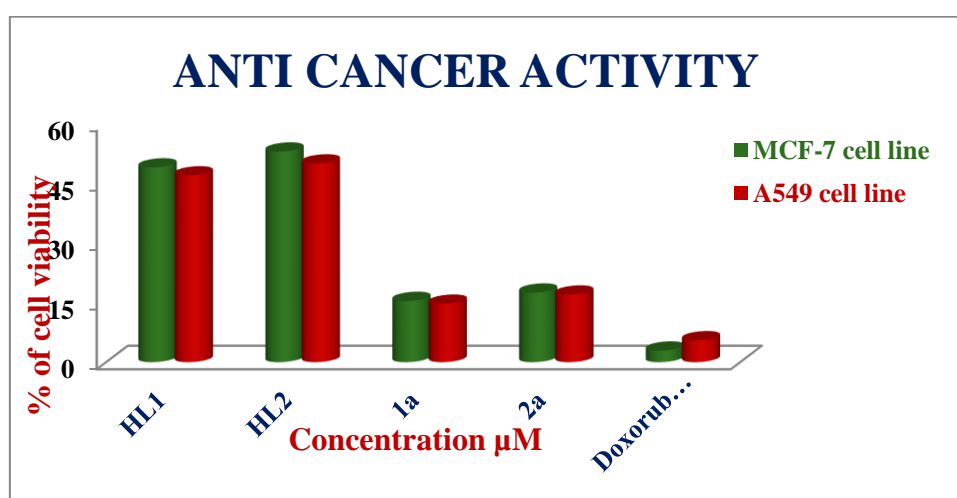


Figure 10. anticancer activity of Schiff bases (HL<sub>1</sub> & HL<sub>2</sub>) and their metal complexes (1a & 2a) against MCF-7 and A549 cell lines.

## 4. CONCLUSION:

Three novel Schiff base metal complexes 1a and 2a have been synthesized from a Schiff base ligands HL<sub>1</sub> and HL<sub>2</sub>, which is characterized by elemental analysis and spectral analysis such as FT-IR, UV-Vis, Mass, and TGA, which revealed that the Zn(II) complexes exhibited an octahedral geometry, coordination water molecule is present in the Zn(II) complexes which were confirmed by FT-IR and TGA. DNA interaction studies revealed that two synthesized complexes bind via intercalative mode. DNA cleavage studies concluded that the synthesized Zn(II) complexes cleaved into nicked form in both cleavage modes. Biological studies performed by antimicrobial, and cytotoxicity have shown that the 1a complex have shown enhanced activity compared to a complex and their respective ligands.

### ACKNOWLEDGEMENTS:

We would like to express our sincere thanks to the Head, Department of Chemistry for providing the necessary facilities for carrying out the work successfully. We are thankful to Director, CFRD, Osmania University and the Director, NITW for providing spectral and analytical data.

### REFERENCES:

- [1] McQuitty, R.J. Metal-based drugs. *Sci. Prog.* 2014, 97, 1–19. [CrossRef] [PubMed]
- [2] Sodhi, R.K. Metal Complexes in Medicine: An Overview and Update from Drug Design Perspective. *Cancer Ther. Oncol. Int. J.* 2019, 14.
- [3] Gali Ramesh, Sreenu Daravath, M Swathi, V. Sumalatha, Dasari Shiva Shankar, Shivaraj. Investigation on Co(II), Ni(II), Cu(II) and Zn(II) complexes derived from quadridentate salen-type Schiff base: Structural characterization, DNA interactions, antioxidant proficiency and biological evaluation. *Chemical Data Collections.* 28(2020) 100434.
- [4] Liu, X.; Hamon, J.R. Recent developments in penta-, hexa- and heptadentate Schiff base ligands and their metal complexes. *Coord. Chem. Rev.* 2019, 389, 94–118.
- [5] Sarker, D.; Karim, M. R.; Haque, M. M.; Zamir, R.; Asraf, M. A., Copper (II) Complex of Salicylaldehyde Semicarbazone: Synthesis, Characterization and Antibacterial Activity. *Asian Journal of Chemical Sciences.* 2019, 1-8.
- [6] Sarker, D.; Reza, M. Y.; Haque, M. M.; Zamir, R.; Asraf, M. A., Synthesis, Characterization, Antibacterial and Thermal Studies of Cu (II) Complex of Thiophene-2-aldehyde Semicarbazone. *Asian Journal of Applied Chemistry Research.* 2019, 1-10.
- [7] Ndagi, U.; Mhlongo, N.; Soliman, M.E. Metal complexes in cancer therapy - an update from drug design perspective. *Drug design, development and therapy* 2017, 11, 599-616,
- [8] Shahabadi, N.; Mohammadi, S. Synthesis Characterization and DNA Interaction Studies of a New Zn(II) Complex Containing Different Dinitrogen Aromatic Ligands. *Bioinorganic Chemistry and Applications* 2012, 2012, 1-8,
- [9] Bastaki A, *Inter J Diabetes Metab*, 13 (2005) 111.
- [10] Whitcomb D C & Lowe M E, *Dig Dis Sci*, 52 (2007) 1.
- [11] M. A. S. Omer, J. Liu, W. Deng, N. Jin, *Polyhedron* 2014, 69, 10
- [12] A. A. Maihub, U. K. Mahanta, G. Badhei, R. K. Mohapatra, P. K. Das, *Rasayan J. Chem.* 2018, 11, 166.
- [13] E. Pahonțu, D. C. Iliș, S. Shova, C. Paraschivescu, M. Badea, A. Gulea, T. Ros, *Molecules* 2015, 20, 5771.
- [14] L. Kelland, The resurgence of platinum-based cancer chemotherapy, *Nat. Rev. Cancer* 7 (2007) 573–584.
- [15] S. Van Zutphen, J. Reedijk, Targeting platinum anti-tumour drugs: overview of strategies employed to reduce systemic toxicity, *Coord. Chem. Rev.* 249 (2005) 2845–2853.
- [16] R.W.Y. Sun, C.M. Che, The anti-cancer properties of gold(III) compounds with dianionic porphyrin and tetradentate ligands, *Coord. Chem. Rev.* 253 (2009) 1682–1691.
- [17] Sreenu Daravath, Aveli Rambabu, Narendrula Vamsikrishna, Nirmala Ganji & Shiva Raj. Synthesis, structural characterization, antioxidant, antimicrobial, DNA incision evaluation and binding investigation studies on copper(II) and cobalt(II) complexes of benzothiazole cored Schiff bases. *J C Chem. Volume 7, 12 (2019) 1973-1993.*
- [18] Sreenu Daravath, Narendrula Vamsikrishna, Nirmala Ganji, Kadatala Venkateswarlu, Shivaraj. Synthesis, characterization, DNA binding ability, nuclease efficacy and biological evaluation studies of Co(II), Ni(II) and Cu(II) complexes with benzothiazole Schiff base. *Chem Data Coll.* 17–18 (2018) 159-168.
- [19] L.C. Jean, Density-functional theory of atoms and molecules. *Int. J. Quantum Chem.* 47 (1993) 101.
- [20] K. Jagadesh babu. SYNTHESIS AND BIOLOGICAL PROFILING OF ZN(II) COMPLEXES WITH 6-AMINOBENZOTHIAZOLE-DERIVED SCHIFF BASES: INSIGHTS INTO DNA BINDING AND SPECTROSCOPIC PROPERTIES. *J Emer Tech Inn Res.* 13(4) 2026.
- [21] Razeq SEAE, Gamasy SME, Hassan H, Aziz MSA, Nasr SM. Transition metal complexes of a multidentate Schiff base ligand containing guanidine moiety: Synthesis, characterization, anti-cancer effect, and anti-microbial activity. *J Mol Structure* (2020); 12381.
- [22] K Jagadesh babu, Synthesis, Spectroscopic Characterization, DNA Binding, and Biological Evaluation of Zn(II) Complexes Derived from 5-Cyclohexylaminedine-Based Schiff Bases, *Volume - 11, 62 (2025) 194-205.*
- [23] Gopichand K, Mahipal V, Rao NN, Ganai AM, Rao PV. Co(II), Ni(II), Cu(II), and Zn(II) complexes with Benzothiazole Schiff base ligand: Preparation, Spectral Characterization, DNA Binding, and In Vitro Cytotoxic Activities *Res in Chem* 5,(2023), 100868. <https://doi.org/10.1016/j.rechem.2023.100868>. [24] Subastri A, Durga A, Harikrishna K, Sureshkumar M, K Jeevaratnam, Girish KS, Thirunavukkarasu C. Exploration of disulfiram dealings with calf thymus DNA using spectroscopic, electrochemical and molecular docking techniques. *J Lumin* (2016); 170:255-261.
- [25] Kumar MP, Ayodhya D, Shivaraj. Novel copper (II) binary complexes with N,O-donor isoxazole Schiff base ligands: Synthesis, characterization, DPPH scavenging, antimicrobial, and DNA binding and cleavage studies. *Res Chem* 5 (2023), 100845.
- [26] Nakamoto K. *Infrared and Raman Spectra of Inorganic and Coordination Compounds.* Wiley-Interscience (1997), 5.
- [27] Devi J, Yadav M, Kumar A, Kumar A. Synthesis characterization biological activity and QSAR studies of transition metal complexes derived from piperonylamine Schiff bases. *Chemical papers* (2018); 72: 2479–2502.
- [28] Ramadan M. Ramadan, Amr M. A. Naeem, Amir E. Aboelhasan, and Ayman A. Abdel Aziz. DNA Binding and Antioxidant Activities of Novel Synthesized Fe(III), Ni(II) and Cu(II) Complexes Derived from Monodentate V-Shaped Schiff Bases. *Journal of Transition Metal Complexes.* 7 (2024) 246166.
- [29] Gali Ramesh, Sreenu Daravath, K. Jagadesh Babu, Ravinder Dharavath, Amit Ranjan, Dasari Ayodhya, Shivaraj. Design, Synthesis, Structural Investigation and Photo Induced Biological Investigations of Co(II), Ni(II) and Cu(II) Complexes Derived from N,O Donor Schiff Bases. *J. Flu* 34 (2024) 2087–2108.
- [30] Kumar MP, Vamsikrishna N, Ramesh G, Subhashini NJP, Nanubolu JB & Shivaraj. Cu(II) complexes with 4-amino-3,5-dimethyl isoxazole and Aromatic aldehyde Schiff bases: synthesis, crystal structure, antimicrobial activity, DNA binding and cleavage studies. *J.C.Chem* (2017); 70, 1368-1388
- [31] N. Jyothi, Sreenu Daravath, M. Swathi, K Jagadeshbabu, Nirmala Ganji, Shivaraj. Synthesis, geometry optimization and non-isothermal kinetic parameters of copper(II), nickel(II) and cobalt(II) complexes of 5-(trifluoromethyl)-2-methoxybenzenamine: DNA binding, cytotoxicity, antioxidant and antimicrobial



## Supplementary Information

### Figures with Captions

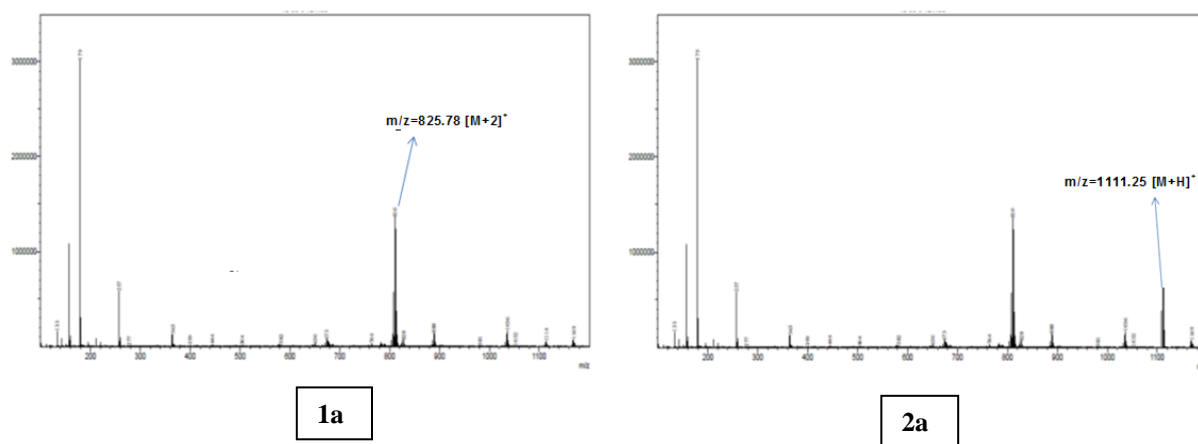


Figure 3. ESI- Mass spectrum (positive ion mode) of the metal complexes **1a**, and **2a**.

### Table form

Table: 1. some notable IR frequencies ( $\text{cm}^{-1}$ ) of Schiff base ligand and its metal complexes.

| COMPOUND | $\nu(\text{O} - \text{H}) \text{ cm}^{-1}$ | $\nu(\text{C} = \text{N}) \text{ cm}^{-1}$ | $\nu(\text{C} - \text{O}) \text{ cm}^{-1}$ | $\nu(\text{M} - \text{O}) \text{ cm}^{-1}$ | $\nu(\text{M} - \text{N}) \text{ cm}^{-1}$ |
|----------|--|--|--|--|--|
| HL1      | 3466                                       | 1611                                       | 1255                                       |  |  |
| HL2      | 3451                                       | 1621                                       | 1152                                       |  |  |
| 1a       | 3438<br>(835, 765)                         | 1617                                       | 1243                                       | 527  | 472  |
| 2a       | 3456<br>(831, 734)                         | 1615                                       | 1138                                       | 553  | 467  |

Table: 2. magnetic momentum and electronic spectra of schiff base and its metal complexes 1a, 1b and 1c.

| COMPOUND | $\pi - \pi^*$                    | $n - \pi^*$                      | CT bands                         | $\mu_{\text{effect}}$ |
|----------|----------------------------------|----------------------------------|----------------------------------|-----------------------|
| HL1      | 256<br>(39062 $\text{cm}^{-1}$ ) | 325<br>(30769 $\text{cm}^{-1}$ ) |                                  |                       |
| HL2      | 261<br>(38314 $\text{cm}^{-1}$ ) | 324<br>(30864 $\text{cm}^{-1}$ ) |                                  |                       |
| 1a       | 261<br>(38314 $\text{cm}^{-1}$ ) | 330<br>(30303 $\text{cm}^{-1}$ ) | 436<br>(22935 $\text{cm}^{-1}$ ) | 0                     |
| 2a       | 265<br>(38910 $\text{cm}^{-1}$ ) | 334<br>(29940 $\text{cm}^{-1}$ ) | 476<br>(21008 $\text{cm}^{-1}$ ) | 0                     |

Table: 3. Schiff base and metal complex antibacterial activity as inhibition zone diameters (mm) at 100  $\mu\text{g}/\text{ml}$  concentration.

| COMPOUND               | GRAM POSITIVE BACTERIUM |          | GRAM NEGATIVE BACTERIUM |              |
|------------------------|-------------------------|----------|-------------------------|--------------|
|                        | B.subtilis              | S.aureus | E.coli                  | K.pneomoniea |
| HL <sub>1</sub>        | 3.1                     | 3.7      | 4.5                     | 4.8          |
| HL <sub>2</sub>        | 2.9                     | 3.5      | 3.8                     | 4.3          |
| 1a                     | 11.3                    | 12.6     | 12.6                    | 13.6         |
| 2a                     | 9.7                     | 10.8     | 10.7                    | 11.5         |
| GENTAMYCIN<br>SULPHATE | 29.1                    | 31.6     | 30                      | 29.3         |

**Table: 4.** Schiff's base and metal complex antifungal activity as inhibition zone diameters (mm) at 100 µg/ml concentration.

| COMPOUND        | A.niger | C.albicans |
|-----------------|---------|------------|
| HL <sub>1</sub> | 10.2    | 10.5       |
| HL <sub>2</sub> | 9.7     | 9.8        |
| 1a              | 20.5    | 20.8       |
| 1b              | 18.4    | 18.9       |
| Nystatin        | 29.8    | 26.1       |

**Table:5.** Anticancer activity of schiff base and its metal complexes against MCF-7 (human breast cancer cell line) and A-549 (human lung adenocarcinoma cell line).

| Compound        | IC <sub>50</sub> (MCF-7) | IC <sub>50</sub> (A549) |
|-----------------|--------------------------|-------------------------|
| HL <sub>1</sub> | 49                       | 47                      |
| HL <sub>2</sub> | 53                       | 50                      |
| 1a              | 15.4                     | 14.7                    |
| 2a              | 17.5                     | 17                      |
| Doxorubicin     | 2.9                      | 5.5                     |